ENEA

Agenzia Nazionale per le Nuove Tecnologie,
l'Energia e lo Sviluppo Economico Sostenibile

Ministero dello Sviluppo Economico

RICERCA DI SISTEMA ELETTRICO

Preliminary Thermohydraulics Design of the LORELEI Device with CATHARE

F.S. Nitti

Report RdS/2011/19

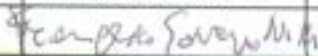PRELIMINARY THERMALHYDRAULIC DESIGN OF LORELEI DEVICE WITH CATHARE
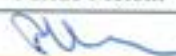
F.S. Nitti (ENEA)

Settembre 2011

Titolo

Preliminary Thermohydraulics Design of the LORELEI Device with CATHARE

Descrittori

Tipologia del documento: **Rapporto Tecnico**

Collocazione contrattuale: Accordo di programma ENEA-MSE:
tema di ricerca "Nuovo nucleare da fissione"

Argomenti trattati: Reattori nucleari ad acqua, Reattori e sistemi innovativi,
Termoidraulica dei reattori nucleari

Sommario

This report has been issued within the framework of the PAR2008-09 research program of the ENEA-MSE agreement and it is one of the deliverables of the task E "Sviluppo e validazione codici di calcolo " of the work program LP2 "Reattori evolutivi".

In the Jules Horowitz Reactor (JHR) experimental facilities are foreseen, including the Light water One Rod Equipment for LOCA Experimental Investigations (LORELEI) device, which is dedicated to Loss Of Coolant Accident (LOCA) transient studies on a single fuel rod.

In this work the thermal-hydraulic design of the LORELEI facility was developed with the code CATHARE. The objective of the work was: to define a 3D geometry of the facility; to verify the capacity of the system, under natural circulation, to remove the power generated by the fuel rod (up to 400 W/cm) and the power generated by gamma irradiation heating on the device materials. The study consisted of three main steps: definition of a 3D geometry of the facility, definition of a numerical model, development of thermo-hydraulic calculations.

Note

This work was developed with CEA – Cadarache Research Center.

Copia n.   In carico a:

2			NOME			
			FIRMA			
1			NOME			
			FIRMA			
0	EMISSIONE	12/09/2011	NOME	Francesco Saverio Nitti	Paride Meloni	Paride Meloni
			FIRMA	Francesco Saverio Nitti		
REV.	DESCRIZIONE	DATA		REDAZIONE	CONVALIDA	APPROVAZIONE

INDEX

FIGURES INDEX

TABLES INDEX

NOMENCLATURE

C_p	specific heat	[J/kg* K]
D_h	hydraulic diameter	[m]
g	gravity acceleration	[m/s^2]
G_r	numero di Grashof	
h	convective coefficient	[W/m^2 K]
k	conductive coefficient	[W/m K]
L	length	[m]
P_r	numero di Prandtl	
Q	heat flux	[W/m^2]
r	radius	[m]
T	temperature	[°C]
T_w	wall temperature	[°C]

α	void fraction	
β	thermal expansion coefficient	[1/°C]
ρ	density	[kg/m^3]
μ	viscosity	[Pa*s]

1. INTRODUCTION

In the Jules Horowitz Reactor (JHR) experimental facilities are foreseen, including the Light water One Rod Equipment for LOCA Experimental Investigations (LORELEI) device, which is dedicated to Loss Of Coolant Accident (LOCA) transient studies on a single fuel rod. The objective of the test device is to evaluate the thermomechanical properties and radiological consequences of LOCA phenomena on a LWR fuel rod.

The system will offer representative conditions to investigate the following phenomena:

- Ballooning and burst of the cladding
- Corrosion phase at high temperature (oxidation and hydration)
- Quenching of the cladding
- Post-quench behaviour of the fuel rod.

The test device will be installed on a displacement system in the core reflector. This arrangement facilitates simple control of fuel rod power by modifying the position of the device from the core. Furthermore, in the case of an accident, this displacement system can ensure safety.

The main operating conditions consist of, [1]:

- Re-irradiation Phase: Before the LOCA transient, the test device is operated as a capsule at below saturation temperature (330,85 °C), in natural circulation, at 13 MPa . These re-irradiation conditions of the fuel sample in the test device create a representative fission product (FP) inventory for radiological purposes or for fuel microstructure studies. The cladding temperature is expected to be similar to PWR temperature ranges.
- Dry-out Phase: The dry-out phase is simulated by a gas injection that allows the emptying of test device to a low pressure value. A small amount of water will remain at the bottom of the device to generate a steam atmosphere during the heat-up phase. The steam will be generated by an electrical heater in the bottom of device.
- Heat-up Phase: The heat-up phase will occur at a rate of 10 to 20°C/s and will be monitored by tuning the power in the fuel. To avoid azimuthal temperature discrepancies, an electrical heating shell will be implemented surrounding the fuel to compensate for azimuthal differences in thermal insulation and thermal inertia. Heating will be stopped at a high temperature in order to increase the apparent heat-losses of the rod and therefore avoid the steam-zircalloy thermal escalation.
  For the power distribution, a neutron screen will be installed to flatten the axial power profile and to reduce, if necessary, the radial profile.
- Quenching Phase: The quenching phase will be simulated by a water injection at the bottom of the test device. It is possible to operate in the long term (several hours or days) at low power which will allow the investigation of post-quench fuel behaviour. Sampling lines are foreseen to analyse FP activities during the post-quench phase. The initial internal rod pressure is a test parameter that can be adjusted, depending on the expected ballooning and burst conditions.

In fig.1 schematic representation of the device, displacement system and its position in the reflector is displayed.
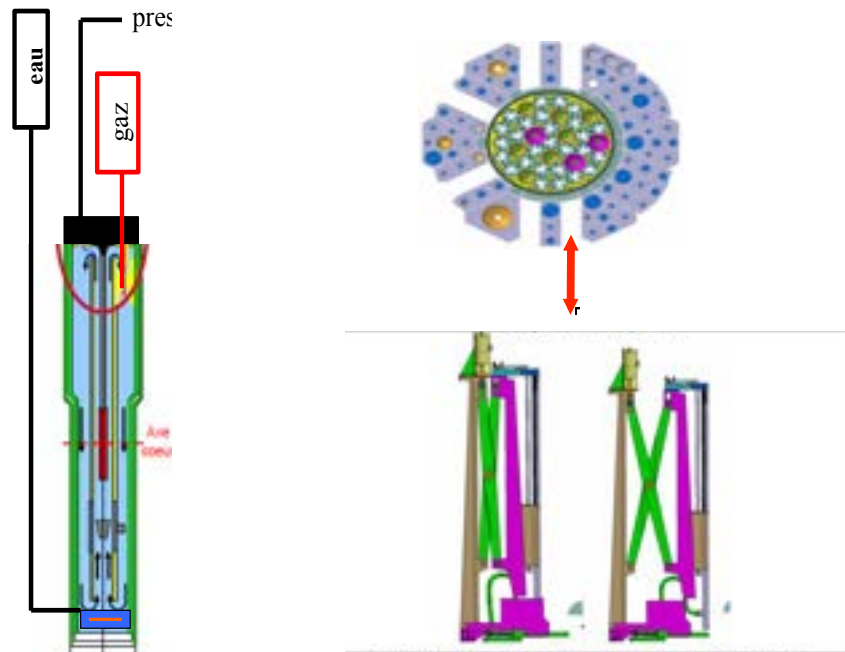
Figure 1 Schematic representation of device, displacement system and its position in the core shield

2. OBJECTIVES

In this work the thermalhydraulic design of the LORELEI facility was developed with the code CATHARE. The objective of the work was:

- to define a 3D geometry of the facility
- to verify the capacity of the system, under natural circulation, to remove the power generated by the fuel rod (up to 400 W/cm) and the power generated by gamma irradiation heating on the device materials

The study consisted of three main steps:

- definition of a 3D geometry of the facility
- definition of a numerical model
- development of thermohydraulic calculations.

3. THE GEOMETRY OF THE FACILITY

In normal operating conditions the LORELEI device operates with pressurized water in natural circulation, moving the generated nuclear thermal power from a hot to a cold well.

Essentially the system is composed of two concentric cylinders with the internal cylinder containing the fuel rod (the hot well) and the external cylinder in contact with a pool (the cold well). The annular chamber between the rod and the internal cylinder is the hot channel, where the heat is removed from the rod, the annular chamber between the two cylinders is the cold channel, where the heat is transmitted to the external pool. However in reality, the system will be composed of cylindrical layers of different materials, which meet different needs in the normal and safety operating conditions. With reference to the schematic cross section of the device displayed in the fig.2, following the description of utilized materials:

- Zircalloy : utilized for the cladding of the fuel rod;
- Zirconia: utilized as a structural material
- Incon 718: utilized as the basic material for the electrical heater. The heater is implemented to compensate azimuthal differences in thermal insulation and thermal inertia, in order to avoid azimuthal temperature discrepancies;
- Porous Zirconia: utilized as a thermal insulation screen between the hot and cold channel
- Hafnium: utilized as a neutron screen installed to flatten the axial power profile and to reduce, if necessary, the radial profile;
- Inox 316: utilized for the external cylinder, which is composed of two cylinders separated by a gas gap. The internal is the first containment wall of the device and the external is the second containment wall for safety purposes. Inox 316 is also used for the water discharge pipe which will simulate the break in LOCA phenomena.
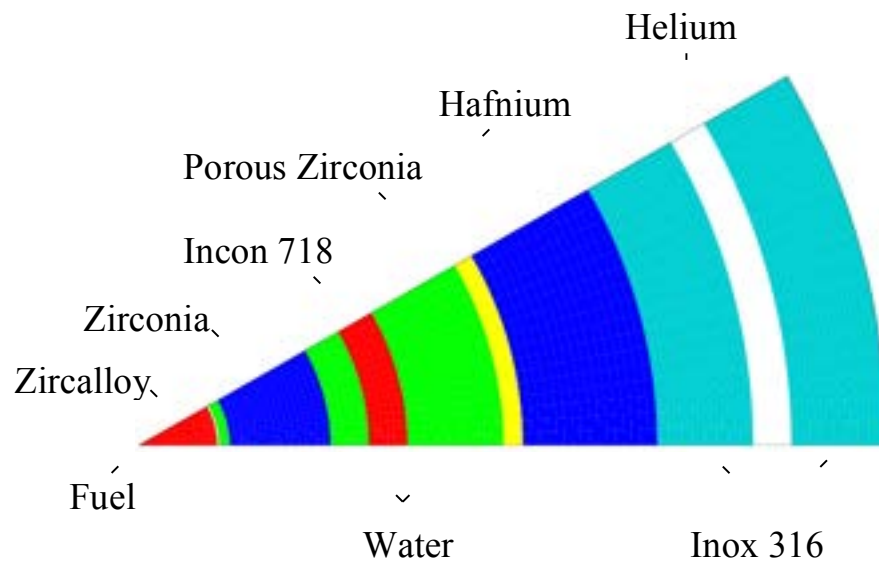
Figure 2 Schematic two-dimensional drawing and materials

The geometry defined in the fig.2, supplied by JHR team, was utilized as a starting point to build a 3D geometry of the facility. In fig.3 and 4 the axial section, cross section and axonometric views are displayed. The connection between the hot and cold channel consist of 4 holes located on a plane and separated 90° from each other.

The drawings were created with SOLID-WORKS software.
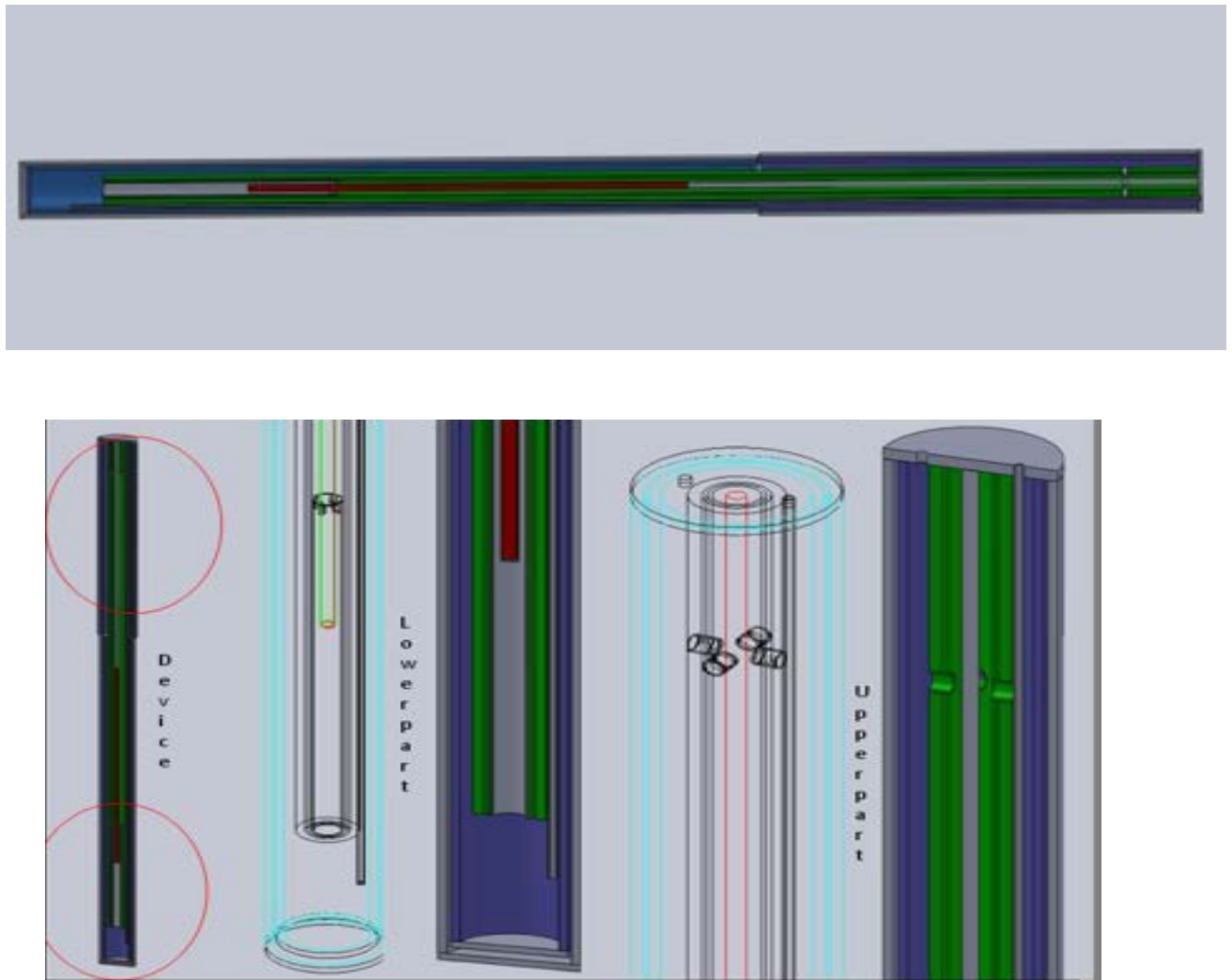
Figure 3 Axonometric views of device
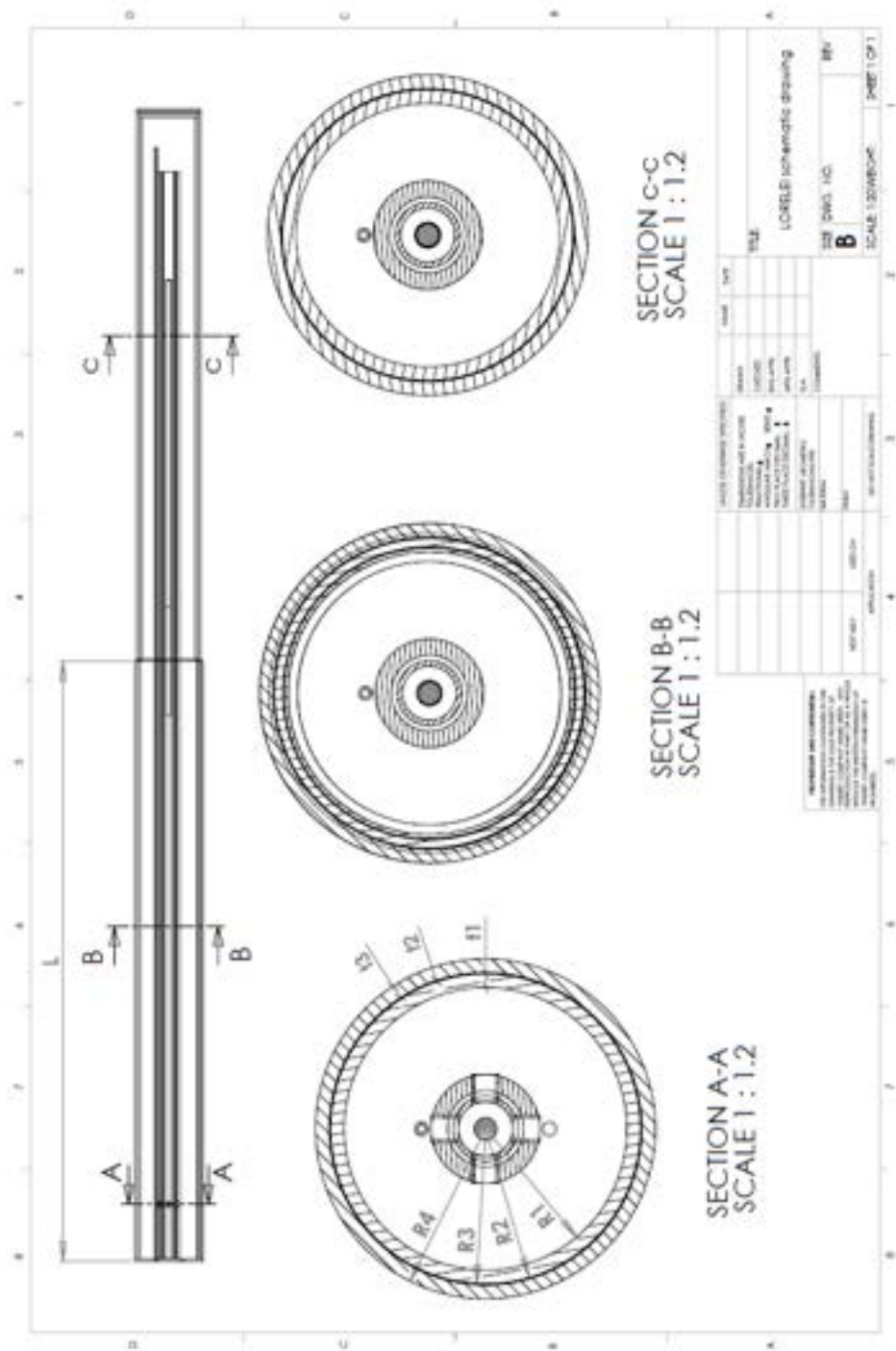
Figure 4 Axial and cross section of device

4. THE NUMERICAL MODEL

The numerical calculations were performed with CATHARE 2 V2.5_2, a two-phase thermohydraulic code with a 2-fluids and 6-equations model. The code resolves three equations per phase: energy, mass and momentum with six principal variables: pressure, enthalpy of liquid and gas, velocity of liquid and gas, void fraction, [2].
The input data required for these calculations were:

- Geometries
- material physical properties (Appendix A)
- local pressure drop coefficients (Appendix B)
- boundary conditions.

Fig.5 displays the discretized model of the system, features include:

- the hot channel (HOTCHAN), upward annular water channel along the fuel rod
- the cold channel (COLCHAN), downward annular water channel in contact with the cold well
- a connection duct (CONHC) to simulate the connection holes between the hot and cold
- channels at the top of device
- the water discharge channel (WATDIS), to simulate the break in the LOCA phenomena
- the lower plenum (LOWPLEN), a volume at the bottom of the device to connect the hot and cold channels.

Typical calculation parameters used were:

- number of meshes: 474
- meshes length: from 1mm to 10 mm
- boundary conditions: pressure 13 MPa, temperature 50 °C on the external wall of device.

Different geometries of the device with different number and length of meshes was studied. The above values are referred to the geometry of the case G5. Some calculations were performed with a double number of meshes to verify the grid independence of results. The variation of calculated physical parameters is negligible, order of variation 0,02 %.

5. THE THERMO-HYDRAULIC CALCULATIONS

There are three main thermohydraulic operational conditions of the device:

- the re-irradiation phase, in which the power generated will be removed in natural circulation conditions
- the dry-out phase, in which the system will be emptied with a gas injection
- the quenching phase, in which the system will be re-flooded with water.

The thermohydraulic calculations were performed for all three operating conditions.
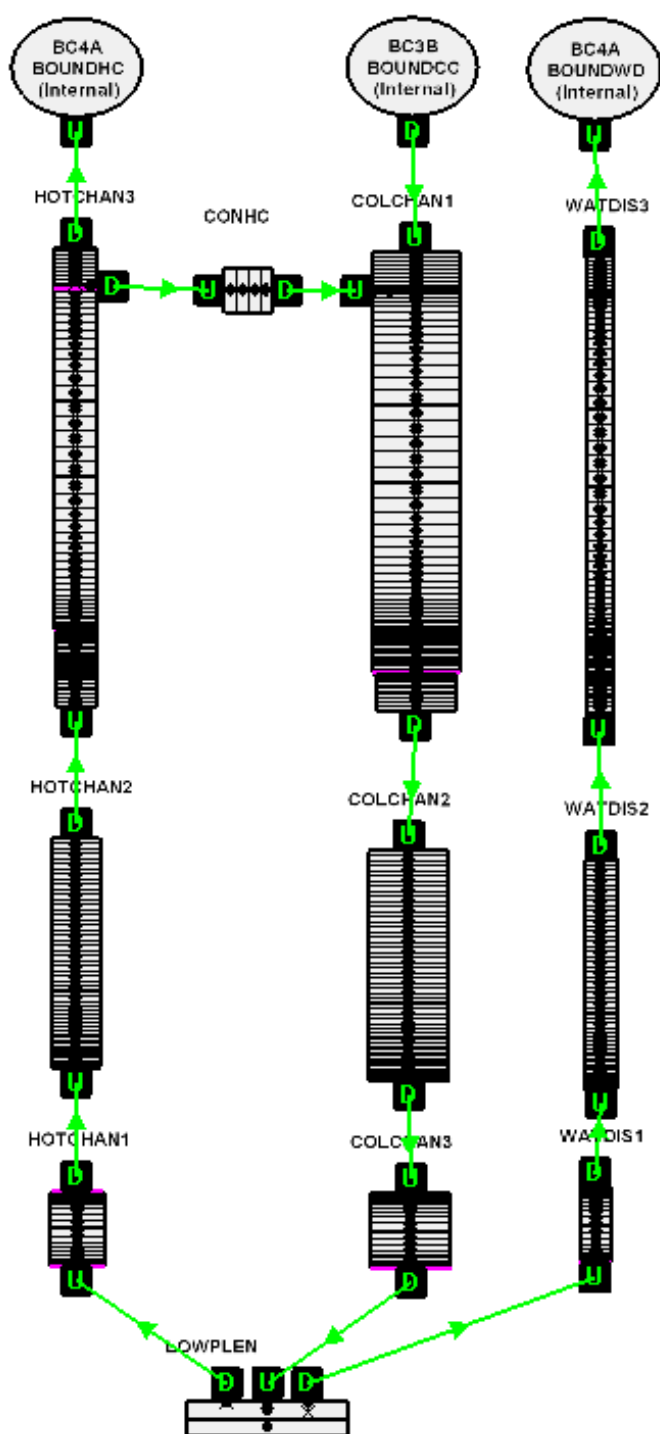
Figure 5 Nodalization of device

5.1 NATURAL CIRCULATION PHASE

The system must operate under natural circulation, moving the thermal power, both produced by fission in the fuel rod and generated by gamma irradiation in the structures, from the device to a cold well of water surrounding the system.

The required operating conditions for this phase are:

- fluid temperature below the saturation value
- cladding temperature above the saturation value, to guarantee nucleation conditions at the wall
- sufficient margin for the Critical Heat Flux (CHF).

Different geometries were analyzed modifying the three parameters: r_1, L, t_2, as displayed in fig. 4. In tab.1 the data of main cases analyzed are displayed. In order to evaluate the impact of the two heat sources the calculation was developed in two steps: the first taking in account only the fission thermal power generated in the rod, the second considering also the thermal power produced by the gamma-heating in the structures.

	r_1 [mm]	L [mm]	t_2 [mm]	Max Power on Fuel Rod [W/cm]	Gamma-Power [W]	$DNBR_{min}$
G0	30.54	700	2	300	-	1.30
G1	50.54	700	2	300	-	1.97
G2	30.54	1200	2	300	-	1.99
G3	30.54	700	1.24	300	-	1.97
G4	50.54	1200	1.24	400	-	2.67
G5	52.04	1200	0.5	400	$3.98*10^4$	2.73

Table 1 Data of main cases analyzed

PRELYMINARY ANALYSIS: THERMAL POWER IN FUEL ROD

The first calculation is related to the initial geometry, case G0. The power generated in the rod can vary from 100 W/cm to 400 W/cm. The code CATHARE cannot directly perform a calculation in natural circulation conditions starting with a null velocity field, thus the calculation was started in forced circulation conditions defining: a mass flow at the inlet of the cold channel and a pressure at the exit of the hot channel and the water discharge channel. When the forced circulation field reaches a stable condition, the mass flow is cut-off and natural circulation is developed, with the defined pressure boundary conditions. The simulation showed that the system operates with the max flow temperature below the saturation value only with a generated power less than 100 W/cm. With a bigger power, a large quantity of steam is generated in the device and this does not guarantee continuous and efficient natural circulation. In fig. 6 the void fraction distribution for a rod with linear power of 300 W/cm is displayed. The calculation showed that the system is able to remove the

thermal power from the hot well, however a lot of steam is accumulated in the upper part of the cold channel. The maximum temperature on the clad was 335.8°C.
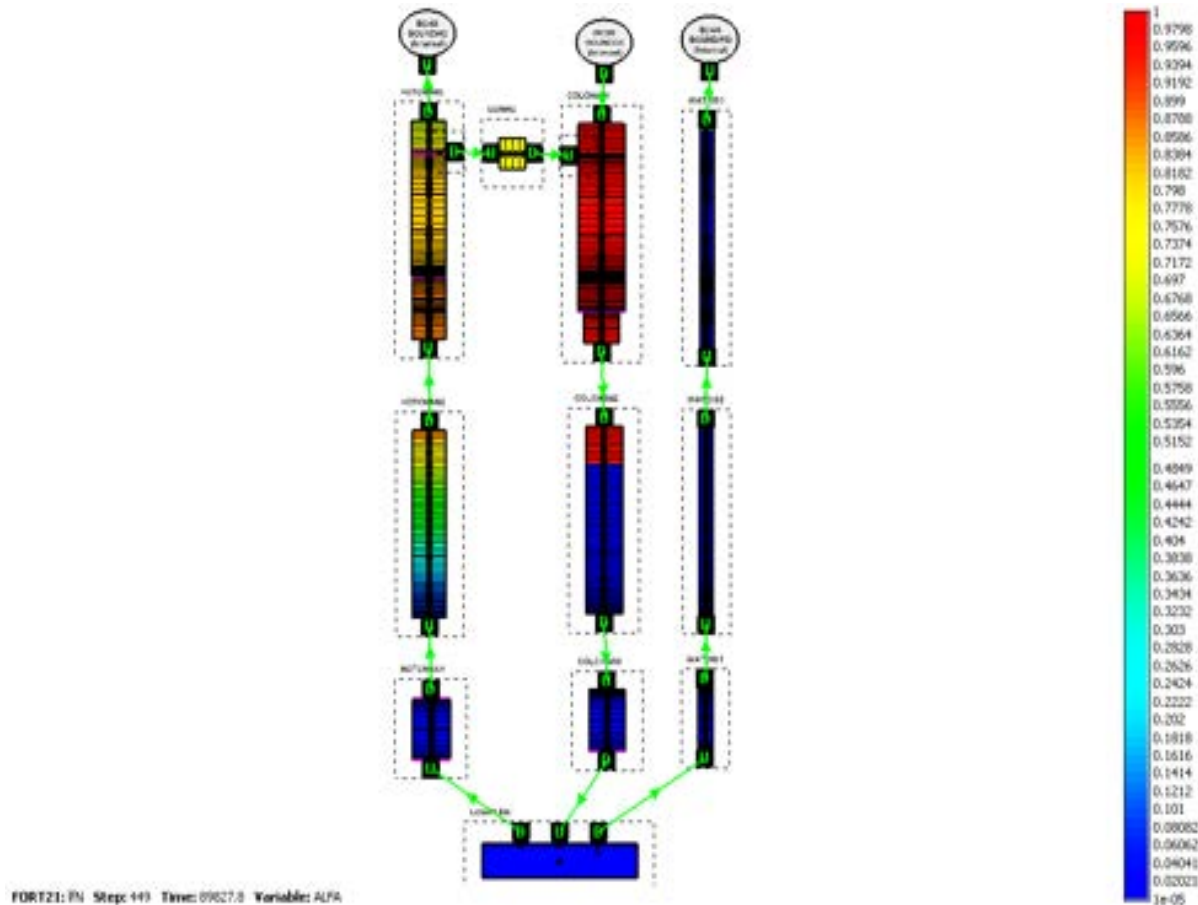
Figure 6 Void fraction distribution with a power of 300W/cm

Evidently it is necessary to increase the heat exchanged with the cold well to reduce the steam production in the device.

The heat exchanged between the cold channel and the surrounding depends on the motion field, geometrical characteristics of the external walls and the surrounding conditions. The surrounding conditions are fixed and the motion field, at fixed power supply, depends on geometrical characteristics of the walls. Therefore a parametric calculation, to analyze the behaviour of the device with variation of geometry, was performed. Keeping constant the geometry of internal cylinder of device, the heat exchange with surrounding is correlated to the geometry of the external cylinder, fig 4: internal and external radius of first wall (r_1, r_2), internal and external radius of second wall (r_3, r_4) , gas gap between the walls t_2 and device length L. In order to evaluate which parameters should be varied and the magnitude of the variation, an analytical approach with an approximate correlation between the heat exchange and geometrical parameters was developed.

5.1.2 ANALYTICAL APPROACH

The external wall of the device is composed of two concentric cylinders with a gas gap, however, due to the small width, the convection circulation is not taken into account and the gas gap is considered as a conductive material. The heat transfer is convective outside the wall and conductive inside the three layers of the wall. The heat flux between the fluid and wall and through each layer in the wall, can be evaluated with the following equations, fig.4:

$$Q_a = -\frac{2\pi L k_a (T_2 - T_1)}{\ln\frac{r_2}{r_1}} \tag{1}$$

$$Q_b = -\frac{2\pi L k_b (T_3 - T_2)}{\ln\frac{r_3}{r_2}} \tag{2}$$

$$Q_c = -\frac{2\pi L k_c (T_4 - T_3)}{\ln\frac{r_4}{r_3}} \tag{3}$$

$$Q_{fi} = 2\pi L r_1 h_i (T_i - T_1) \tag{4}$$

$$Q_{fe} = 2\pi L r_4 h_e (T_4 - T_e) \tag{5}$$

Arranging these correlations, it is possible to have an expression of heat flux as a function of geometric parameters of conductive and convective coefficients and of temperatures of fluids on both side of the wall:

$$Q = \frac{2\pi L r_1 r_4 h_i h_e}{r_1 h_i + r_4 h_e + r_1 r_4 h_i h_e \left[\frac{1}{k_a}\ln\frac{r_2}{r_1} + \frac{1}{k_b}\ln\frac{r_3}{r_2} + \frac{1}{k_c}\ln\frac{r_4}{r_3}\right]}(T_i - T_e) \tag{6}$$

The convective coefficient can be expressed as a function of non-dimensional parameters. In literature several correlations are reported. In the operating conditions of the device, a laminar flow in natural circulation is assumed, and the convective coefficient is evaluated by the following correlation, [3]:

$$h_l = \frac{k_l}{D_{hl}} h(\alpha) 0,55 (Gr_l \, \text{Pr}_l)^{1/4} \tag{7}$$

with

$Gr_l = \dfrac{g\beta_l \rho_l^2 D_{hl}^3}{\mu_l^2}\left\|T_w - T_l\right\|$	$\Pr_l = \dfrac{\mu_l Cp_l}{k_l}$	$\beta_l = -\dfrac{1}{\rho_l}\left(\dfrac{\partial \rho_l}{\partial T_l}\right)_P$
$D_{hl} = D_h\left(1 - R_c\right)$	$R_c = \sqrt{\alpha}\left(1 - Min\left[1, Max\left[\dfrac{2\cdot 10^{-5}}{D_h}, 3\cdot 10^{-3}\right]\right]\right)$	$h(\alpha) = (1-\alpha)/\left(1 - R_c^2\right)$

The CATHARE code utilises a different approach. The convective coefficient of different flow regimes (laminar, turbulent, natural convection, etc.) is evaluated in each mesh by means of correlations and then the maximum value is chosen.

The Global Heat Transfer Coefficient (GHTC) in equation (6) is related to geometrical parameters, and with some simplified hypotheses, it is possible to evaluate its variation with the variation of geometrical parameters.

The CATHARE calculation showed a stable operating condition of the device without steam production, with a linear heat power in the fuel rod less than 100 W/cm. Starting with this stable operating condition, a study was performed to obtain an appropriate global heat transfer coefficient, modifying only the physical dimensions of the device, with the goal of obtaining the same stable conditions of the 100 W/cm case with a bigger linear power supplied. Utilizing the results of the calculation obtained with a power of 100 W/cm, average values for temperatures, density, viscosity, specific heat, conductivity and thermal expansion coefficient, in the cold channel above the rod, were assumed (see tab 2). Assuming that these average physical parameters remain constant, it is possible to calculate the change in the GHTC with the variation of the geometric parameters:

$$k_{tot} = \frac{2\pi L r_1 r_4 h_i h_e}{r_1 h_i + r_4 h_e + r_1 r_4 h_i h_e\left[\dfrac{1}{k_a}\ln\dfrac{r_2}{r_1} + \dfrac{1}{k_b}\ln\dfrac{r_3}{r_2} + \dfrac{1}{k_c}\ln\dfrac{r_4}{r_3}\right]} \tag{8}$$

FLUID		
Temperature	250	[°C]
Density	808,93	[Kg/m3]
Viscosity	1,09E-04	[Pa*s]
Cp	4759,1	[J/kg*K]
Conductivity	0,63239	[W/m*K]
Thermal expansion coefficient	0,005	[1/°C]
Void fraction	10^{-5}	
MATERIALS		
Wall temperature	230	[°C]
Conductivity Iron	15	[W/m*K]
Conductivity Helium	0,22032	[W/m*K]

Table 2 Average physical parameter in the cold-channel above the rod,
as resulted from calculation with linear power of 100 W/cm

Fig.7 displays the variation of GHTC with the variation of internal radius r_1, length L, thickness of first wall t_1, gap between walls t_2, thickness of second wall t_3. These dimensions are displayed in fig. 4. The values on the Cartesian axes are normalized to the initial reference values, tab.1, 2 and drawings in appendix C:

$$k^* = k / k_{int} ; \quad r_1^* = r_1 / r_{1\,int} ; \quad L^* = L / L_{int} ; \quad t_1^* = t_1 / t_{1\,int} ; \quad t_2^* = t_2 / t_{2\,int} ; \quad t_3^* = t_3 / t_{3\,int}. \tag{9}$$

The curves show the percentage increase of heat flux removable from the device, keeping constant the physical condition of the fluid and varying each geometrical parameter one by one. Predictably the gas gap t_2 has a large impact on the variation of GHTC, due to the low conductivity of the gas, while t_1 and t_3 have a low impact. To verify the reliability of these graphs, further CATHARE calculations with different geometries, obtained modifying the three parameters, were performed. In fig.8 the comparison between the variation of normalized GHTCs calculated by the correlation (8) and those obtained from the code calculation is displayed. Code calculation of heat exchange due to L variation is bigger than that calculated by the correlation because the code also evaluated the increase of driving force with increasing of length. In tab.3 the interpolation equations of curves in fig.8 are displayed.
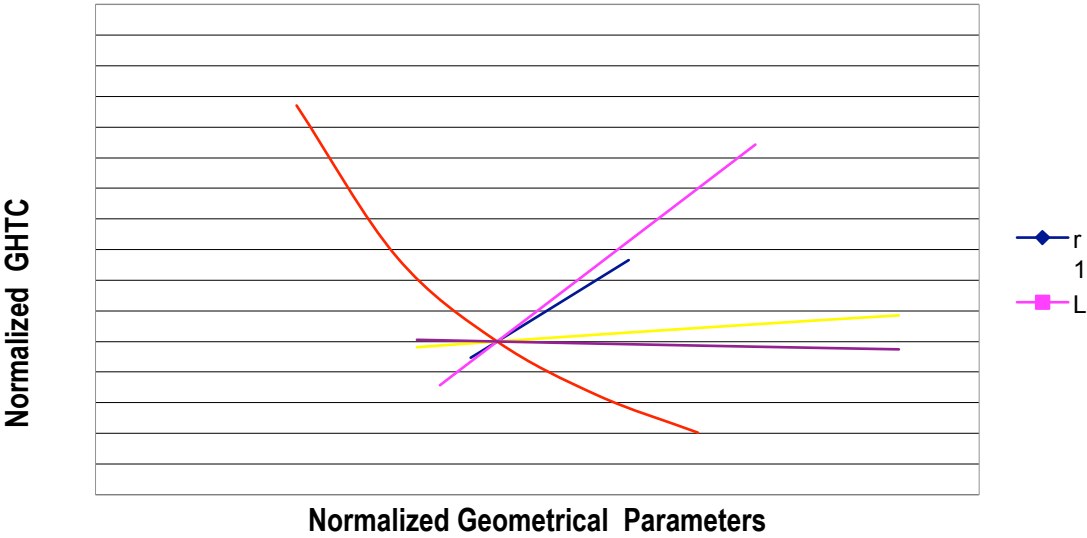
Figure 7 Normalized GHTC as a function of Normalized geometrical parameters
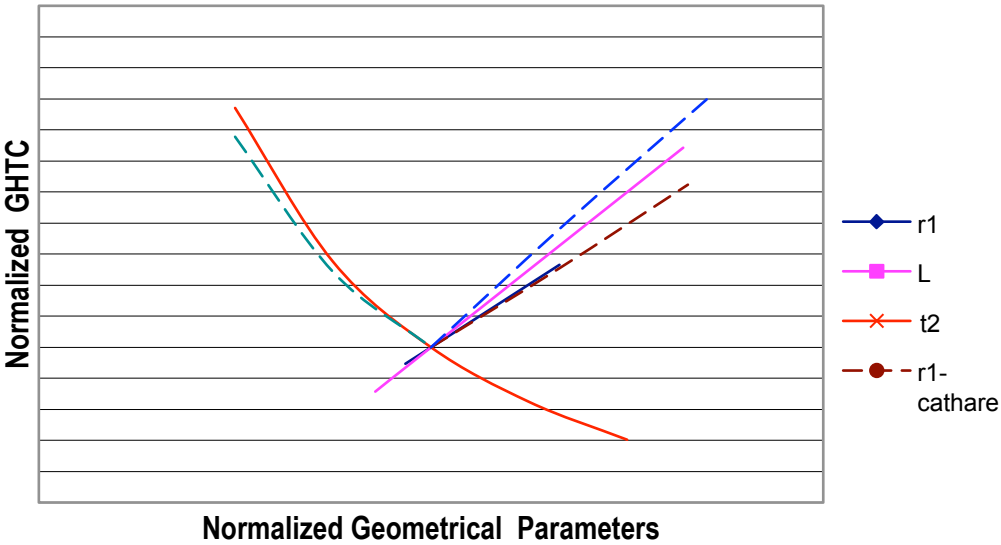
Figure 8 Normalized GHTC as a function of Normalized geometrical parameters.
Calculated by correlation and by CATHARE

	k^*
r_1^*	$y = -2{,}5238\text{E-}03x^2 + 8{,}1858\text{E-}01x + 1{,}8378\text{E-}01$
L^*	$y = x$
t_2^*	$y = 1{,}1812\text{E+}01x^6 - 6{,}2734\text{E+}01x^5 + 1{,}3418\text{E+}02x^4 - 1{,}4913\text{E+}02x^3$ $+ 9{,}3271\text{E+}01x^2 - 3{,}3778\text{E+}01x + 7{,}3810\text{E+}00$

Table 3 Interpolation equations of curves in fig.8

Fluid temperature and void fraction behaviour related to the calculation of some different geometries, tab. 1, in fig.9 and 10 are displayed. Observing the curves in comparison to case G0-300, some considerations is possible to underline. In both cases G1 and G3, a reduction of average temperatures along the system and a reduction of steam production in the colchan1 is showed. Case G2 shows an increase of average temperature in the system (about 10 °C) and an increase of steam production in the colchan1. The variation of length, case G2, does not substantially modified the physics of the heat exchange. The increase of length creates a raise of the driving force and thus velocities and pressure drops. Instead the variation of the other two geometrical parameters acts directly on the physical parameters (Grashof) modifying both the amount of heat exchanged and the physical state condition throughout the system.
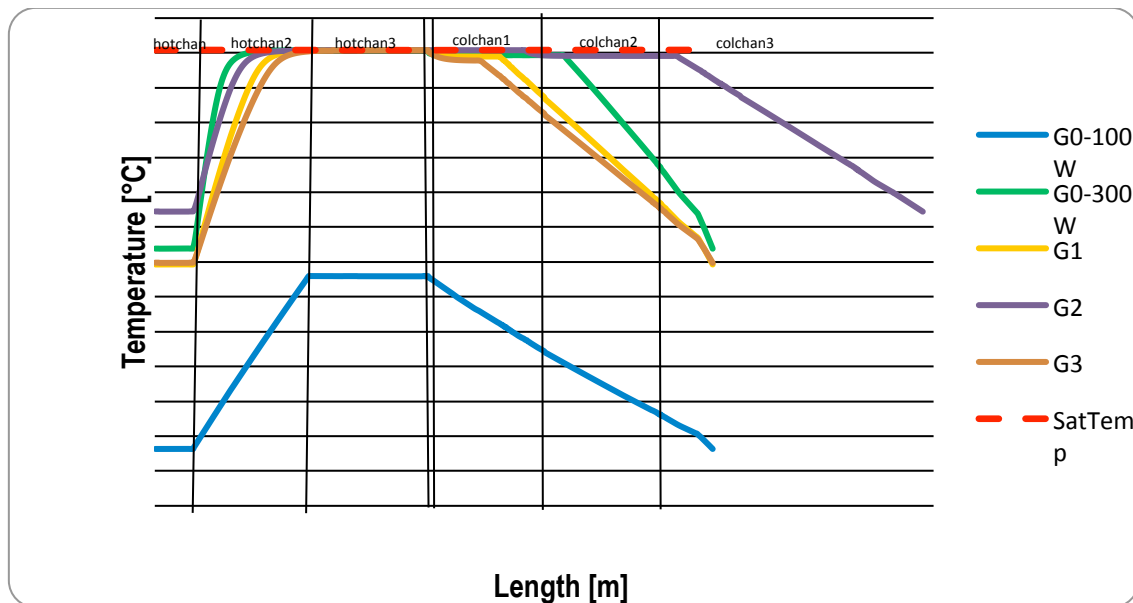
Figure 9 Temperature behaviour for the geometries G0, G1, G2, G3
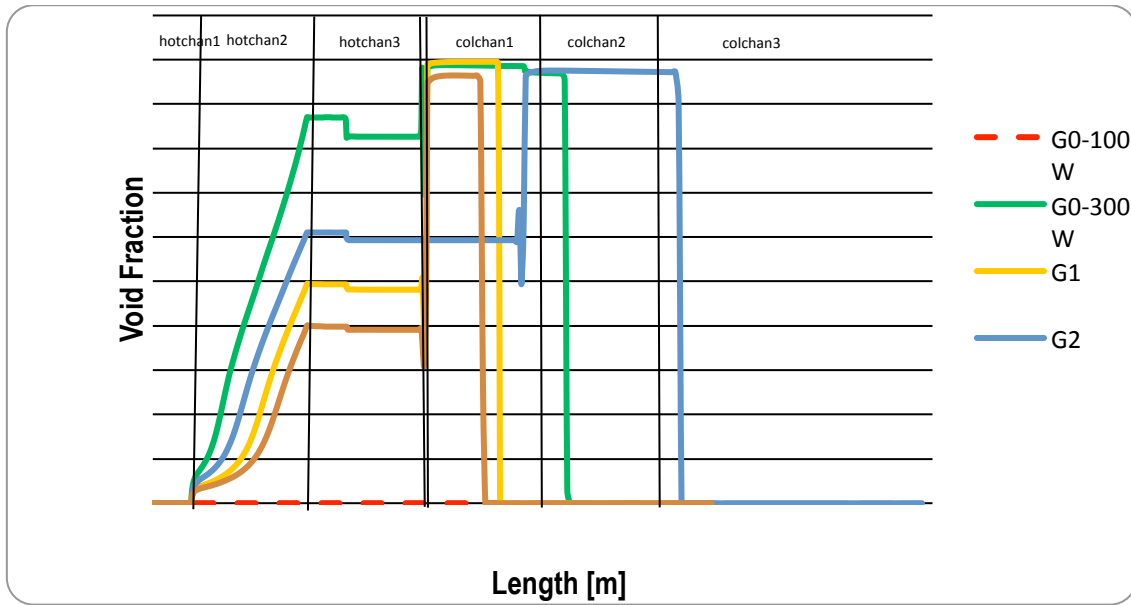
Figure 10 Void fraction behaviour for the geometries G0, G1, G2, G3

SUBSEQUENCE DEVELOPMENT OF CALCULATION

The maximum power that the system should nominally be able to handle is 400 W/cm , four times the initial reference value of 100W/cm. Observing the diagrams in fig.8, the single variation of a geometrical parameter is not enough to guarantee an increased of heat transfer by a factor of four. Therefore a combined variation is necessary.

The curves in fig.8 display the change in GHTC by variation of single parameters, the effect of a combined variation can be evaluated with the hypothesis of principle of superposition of effects and the variation of GHTC can be evaluated by means the correlation:

$$k^* = k_{r_1}^* k_L^* k_{t_2}^*$$

(10)

The GHTC has been expressed as a function of three geometrical variables, thus ∞^3 solutions are possible. The choice must be driven in direction of maximization of the heat exchanged, keeping the system simple, compact and easy manufacture. However the geometrical parameter variation is limited by the space available for the facility (max length 2200 mm and max external diameter 129 mm were assumed in this study), and moreover the gas gap reduction must be limited, to minimize the mechanical problems in the device assembly. Therefore, assuming the maximum values possible for length L and internal radius r_1, the gas gap thickness was calculated. Fixed L and r_1, from (9) the normalized value were calculated, and from the diagrams of fig.8, or by equations in tab.3, the normalized heat transfer

coefficients: $k_{r_1}^*$, k_L^* were determined. Knowing the GHTC required, from (9) the normalized

value was calculated and from (10) the normalized heat transfer coefficients $k_{t_2}^*$ and thus, from the diagram, the gas gap normalized thickness t_2^* , and then t_2. In tab.4 the calculated values are reported.

Geometrical Parameters	r_1	L	t_2
Reference values [mm]	30.54	700	2
Actual values [mm]	50.54	1200	1.24
Normalized values	1.65	1.71	0.62
Normalized GHTC	1.54	1.71	1.52
Total Normalized GHTC	4		

Table 4 Geometrical parameters and normalized values

The calculation with the new geometric parameters, case G4, showed good thermohydraulic behaviour of the system up to 400 W/cm, without a significant amount of steam production. In fig. 11, 12 and 13 the temperature distribution and void fraction behaviour in the fluid are displayed. The diagram in fig.13 show a small quantity of steam in the hot-channel along the rod, thus nucleation phenomena appear in the fluid. This is also underlined from the distribution of temperature on the fuel rod that is over the saturation temperature of the fluid, fig.14, and the non zero value of the heat flux that generates nucleation, fig. 15. The convective flux is the difference between the total flux and nucleate flux.

FORT21: lfdlg1N Step: 361 Time: 90004.4 Variable: LIQTEMP
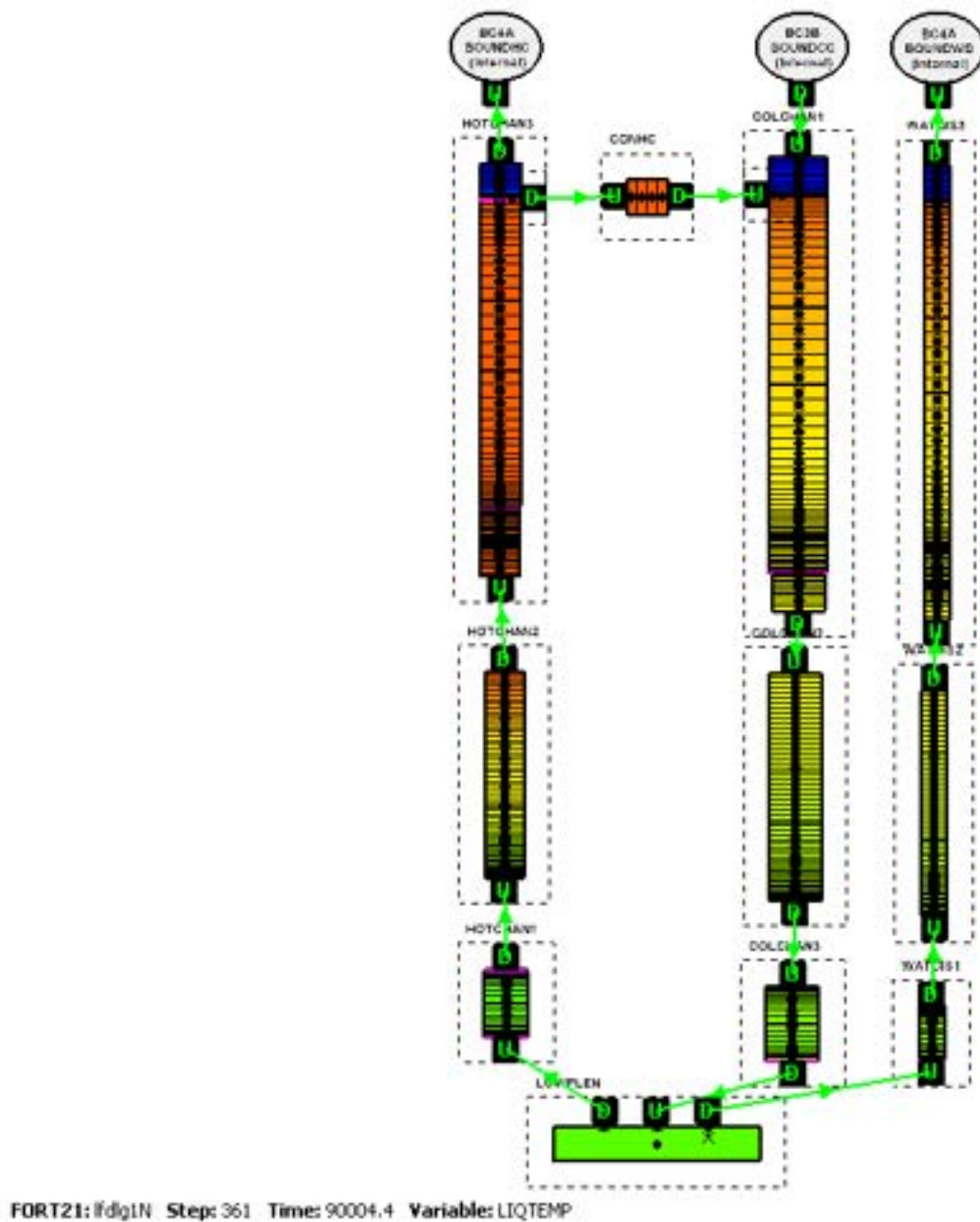
Figure 11 Temperature distribution at linear power of 400 W/cm
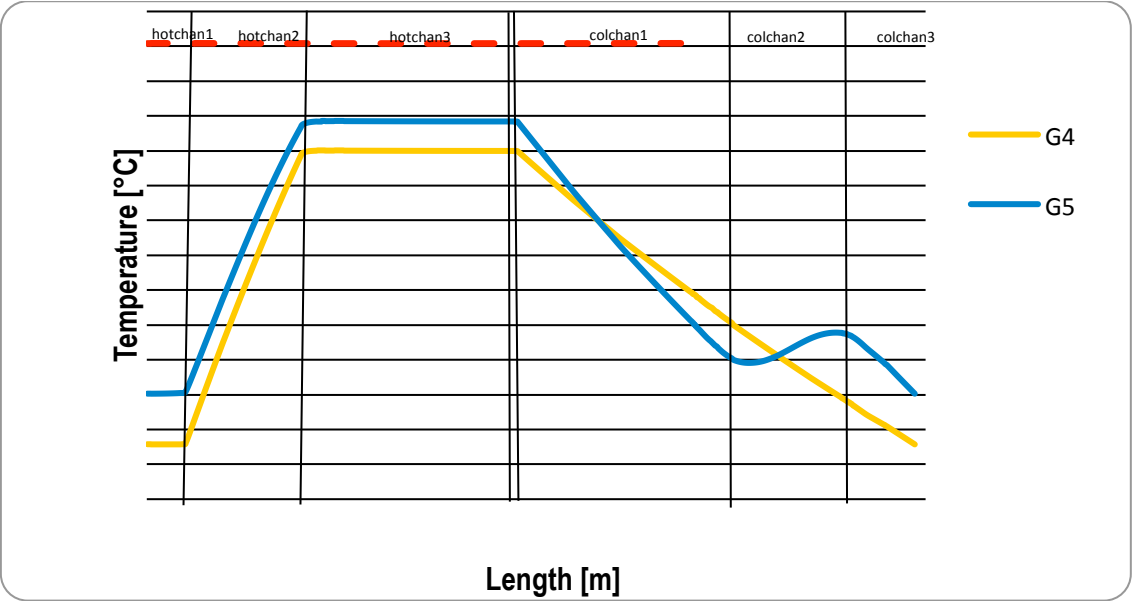
Figure 12 Temperature behaviour for the geometries G4, G5
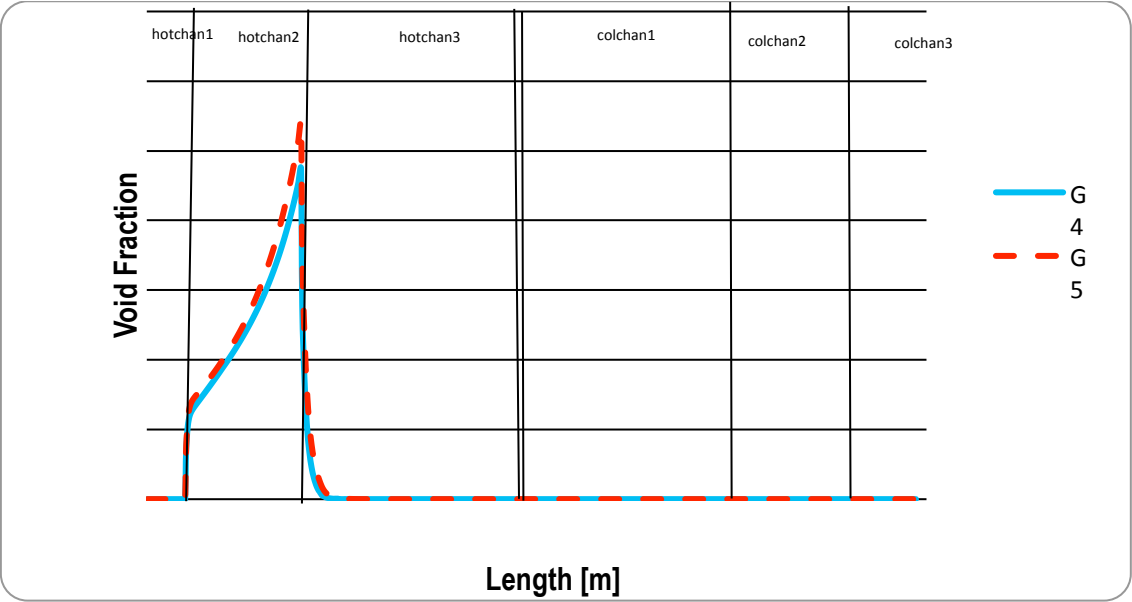
Figure 13 Void fraction behaviour for the geometries G4, G5
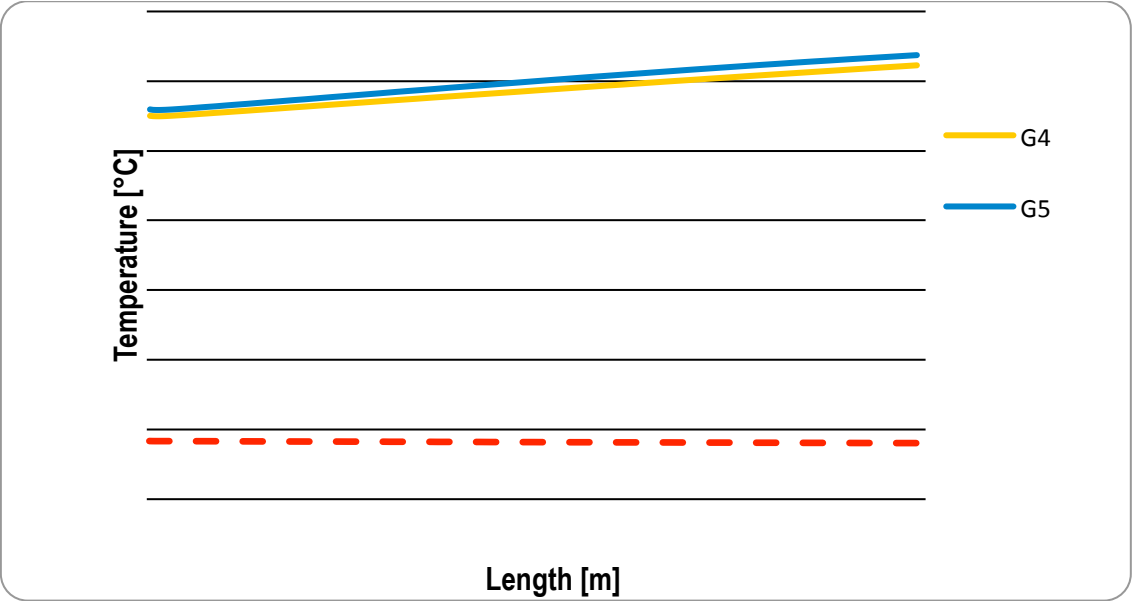
Figure 14 Temperature distribution on the fuel rod for the geometries G4, G5.
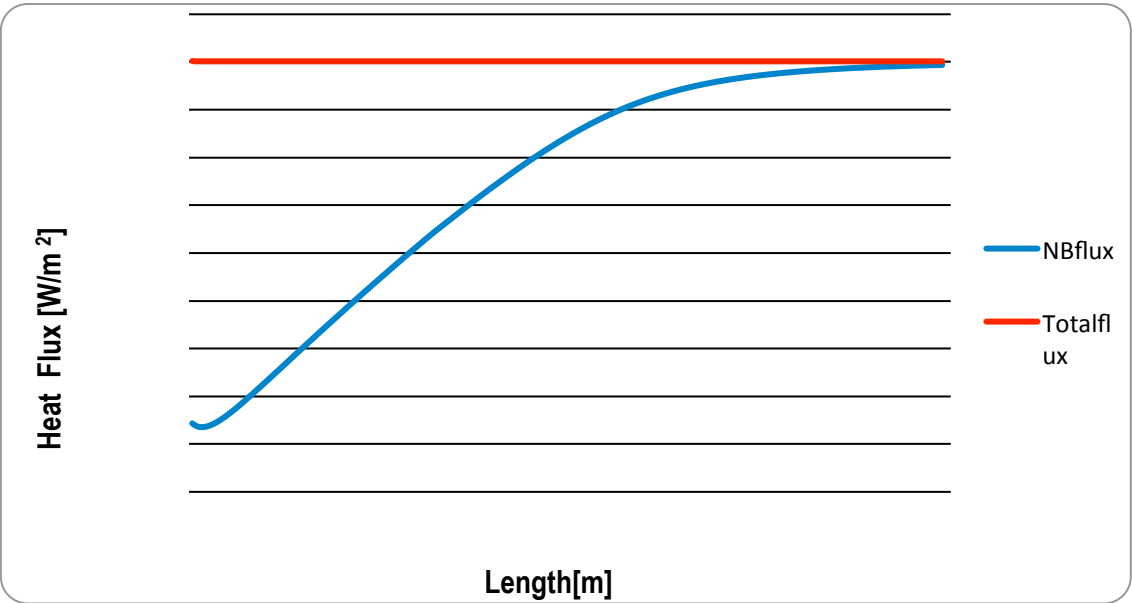
Figure 15 Nucleate Boiling heat flux and Total flux on fuel rod

Fluid temperature below the saturation value is a necessary but not sufficient criterion to guarantee the safe operation of the system. An important parameter that must be satisfied is the Critical Heat Flux (CHF): a heat flux from a wall to the fluid which generates a sudden local evaporation of fluid resulting in a dangerous local superheating of the wall. The CHF is function of field of motion along the wall, in literature several correlations are reported.

The code utilizes the following correlation, [3]:

$$q_{cr} = F1 \cdot F2 \cdot F3 \cdot 10^{F(G,P,\overline{X})+3} \tag{11}$$

With

$F_1 = Max\left(\dfrac{8 \cdot 10^{-3}}{D_h}, 0.79\right)^{1/}$	$F_2 = \begin{cases} 1 & standard \quad value \\ 0.6 & bundle \quad geometr \end{cases}$	$F_3 = \begin{cases} 1 & if \ \overline{X} < 0.9 \\ 10(1-\overline{X}) & if \ \overline{X} \geq 0.9 \end{cases}$
$\overline{X} = \dfrac{\alpha\rho_g + (1-\alpha)\rho_l x}{\alpha\rho_g + (1-\alpha)\rho_l}$	$x = \dfrac{H_l - H_{lsat}(P)}{H_{vsat}(P) - H_{lsat}(P)}$	$G = |G_g| + |G_l| = |\alpha\rho_g V_g| + |(1-\alpha)\rho_l V|$
F is an interpolation function of the GROENEVELD table.		

The ratio between the CHF and the total heat flux on a wall, Departure from Nucleate Boiling Ratio (DNBR), is used to evaluate the risk conditions. Fig. 16 display the DNBR on the fuel rod in the three cases G1, G2 and G3, compared to the case G0. The diagram shows that the margin between the CHF and the total flux is reduced along the rod, moreover the worst behaviour is in the case G2, to confirm the low influence of increased of length on the field of motion. The lowest value of margin from the CHF is equal to two, and the utilized correlation has an uncertainty of about 30%, consequently in these operative conditions the margin is sufficiently good. Fig. 17 display the DNBR on the fuel rod in the case G4, the margin of the CHF is 2.66 on the entire rod.

DNBR

- G0-300 W
- G1
- G2

Length[m]
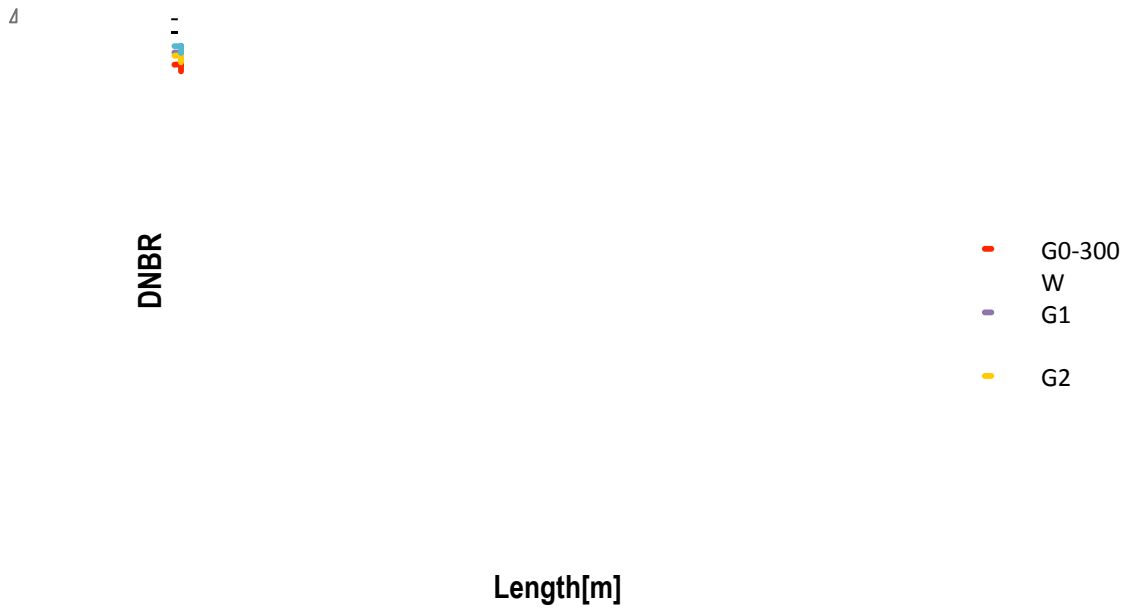
Figure 16 DNBR behaviour for the geometries G0, G1, G2, G3

DNBR

- G4
- G5

Length[m]
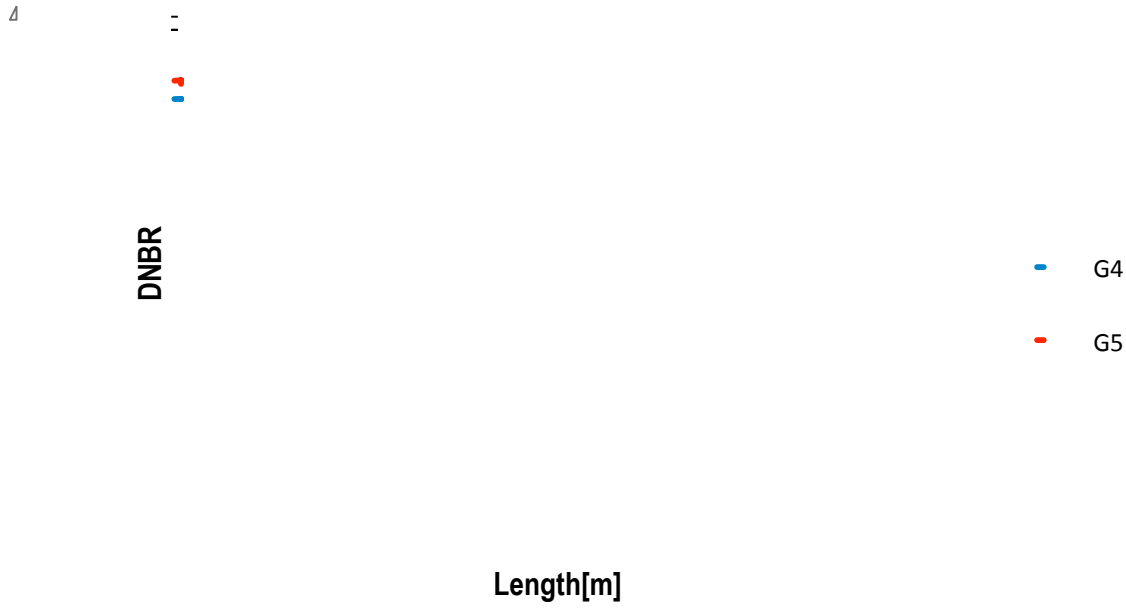
Figure 17 DNBR behaviour for the geometries G4, G5

5.1.4 THERMAL POWER DUE TO GAMMA HEATING

The thermal power generated in the structure of device due to the gamma irradiation constitutes a significant quantity of heat to the system. The amount of gamma-power and its linear distribution was evaluated considering the neutron flux distribution coming from the reactor core, fig. 18. With the hypothesis that the gamma distribution matches the neutron flux distribution, the specific thermal power distribution for each material of the structures of device is evaluated, fig.19. In tab.5 the multiplicative coefficients used to evaluate the maximum gamma heating in materials different from graphite are displayed. The power distribution is centered at the middle of fuel rod and it extends of 200 mm above and below of the rod.
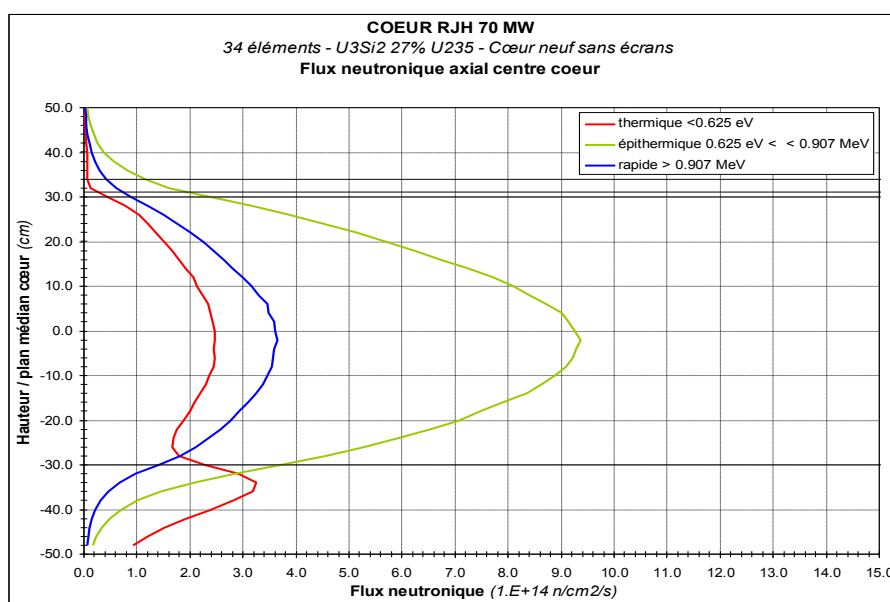
Figure 18 Neutron flux distribution, [4]
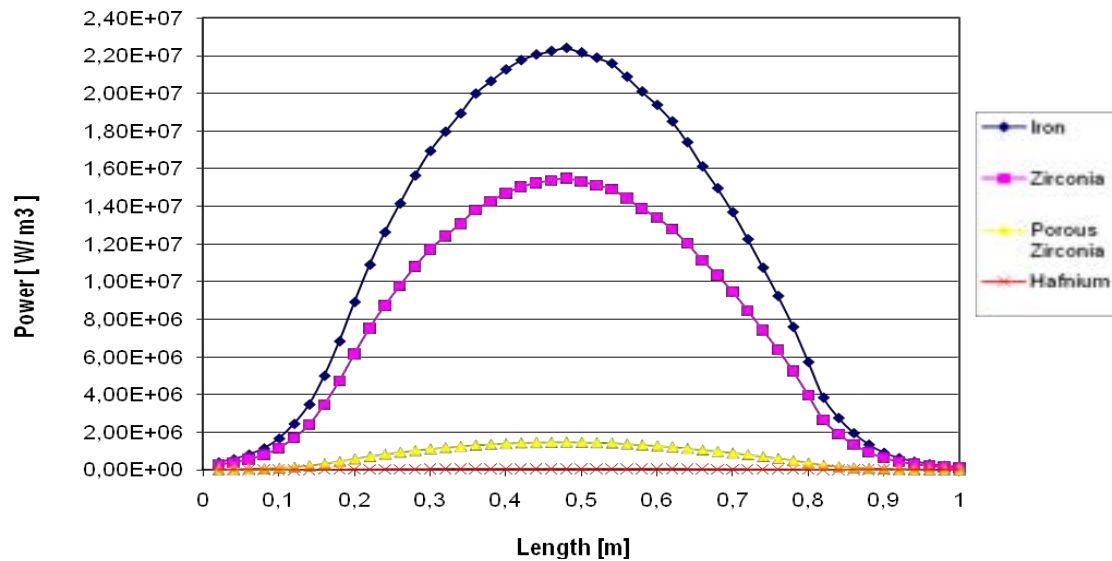
Figure 19 Thermal power due to gamma irradiation

	Variation of specific power $G_{material} / G_{graphite}$	Maximum Gamma Power [W/g]	Density [Kg/m^3]	Maximum Gamma Power [W/m^3]
GRAPHITE	1	2,5		
IRON	1,12	2,8	8000	2,2400E+07
ZIRCONIA	1,23	3,075	5035,8	1,5485E+07
POROUS ZIRCONIA	1,23	3,075	480	1,4760E+06
HAFNIUM	1,73	4,325	13,31	5,7566E+04

Table 5 Correction coefficient and maximum gamma power in the materials, [5]

The thermo-hydraulic calculation in the case G4, considering both the thermal-power in the rod and the gamma-power in the structures, showed a flow field with the presence of steam in the top part of cold channel. The total heat power due to gamma irradiation resulted of about $3.98*10^4$ W distributed on a length of 1 m, therefore it is a linear power distribution of the same order of magnitude of linear power in the rod. Hence it is necessary to change once more the geometry of the device, case G5. The total power, in fuel rod and in structures, is eight times to that of the initial reference geometry; adopting the same procedure presented in the previous paragraph the appropriate gas gap thickness was evaluated. The gas gap reduction was obtained by increasing the internal radius of the wall. The geometrical data variations are reported in tab. 6.

Geometrical Parameters	r_1	L	t_2
Reference values [mm]	30.54	700	2
Actual values [mm]	50.54	1200	0.5
Normalized values	1.65	1.71	0.25
Normalized GHTC	1.54	1.71	3.0
Total Normalized GHTC		8	

Table 6 Geometrical parameters and normalized values related to the final geometry, G5

In fig. 12, 13, 14 and 17 the temperature distribution in the fluid, the void fraction, the temperature distribution along the fuel rod and the DNBR are displayed.

Fig. 20 and 21 show the fluid temperature and DNBR behaviour in the case G5 in relation to different linear powers in the fuel rod and with gamma-heating only on the external walls.
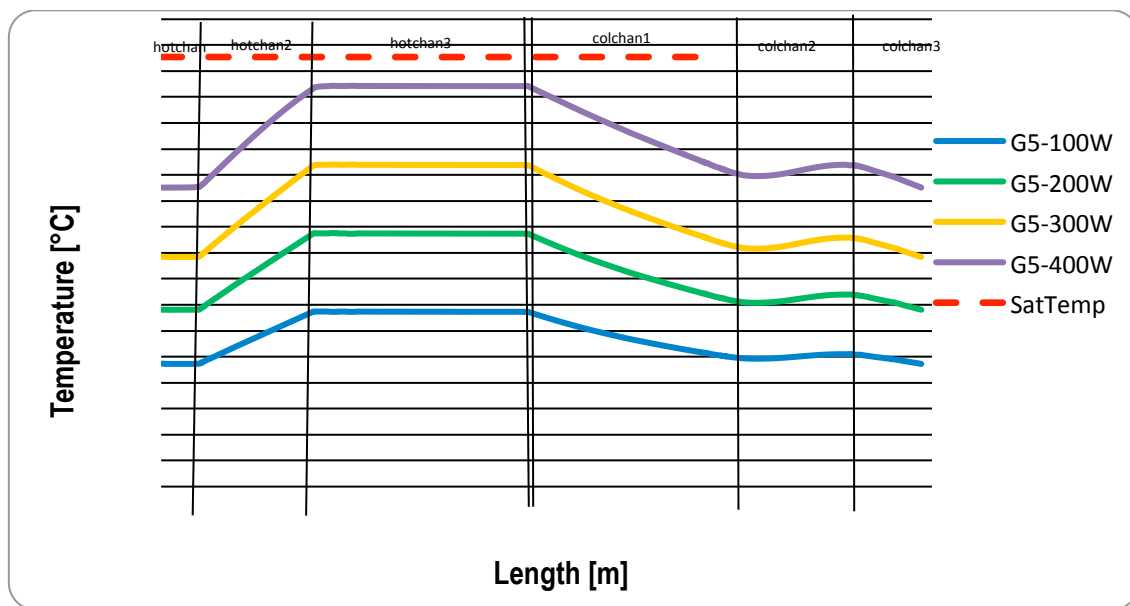
Figure 20 Temperature behaviour at different power, case G5

DNBR

- G5-100W
- G5-200W
- G5-300W
- G5-400W

Lenght [m]
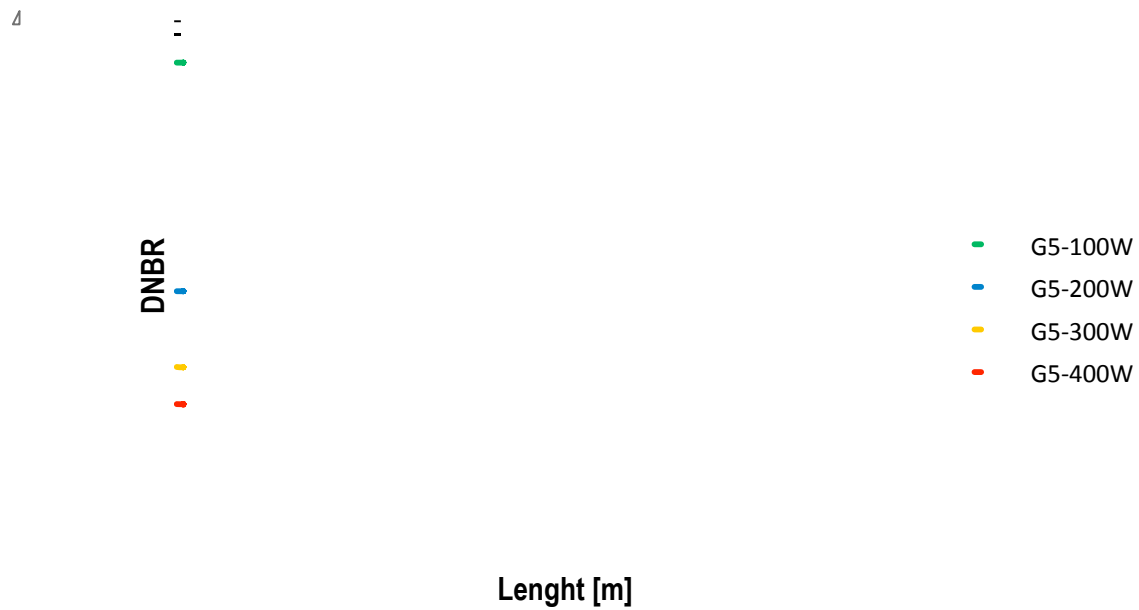
Figure 21 DNBR behaviour at different power, case G5.

Fig.22 displays the heat fluxes through the hot and cold channel, and the heat fluxes between cold channel and external surrounding. The amount of heat flux discharged in the surrounding is about three orders of magnitude to that exchanged between the hot and cold channels. Therefore the wall between the two channels provides sufficient isolation to guarantees an appropriate driving force.

The drawings of the final geometry of device are in Appendix C.
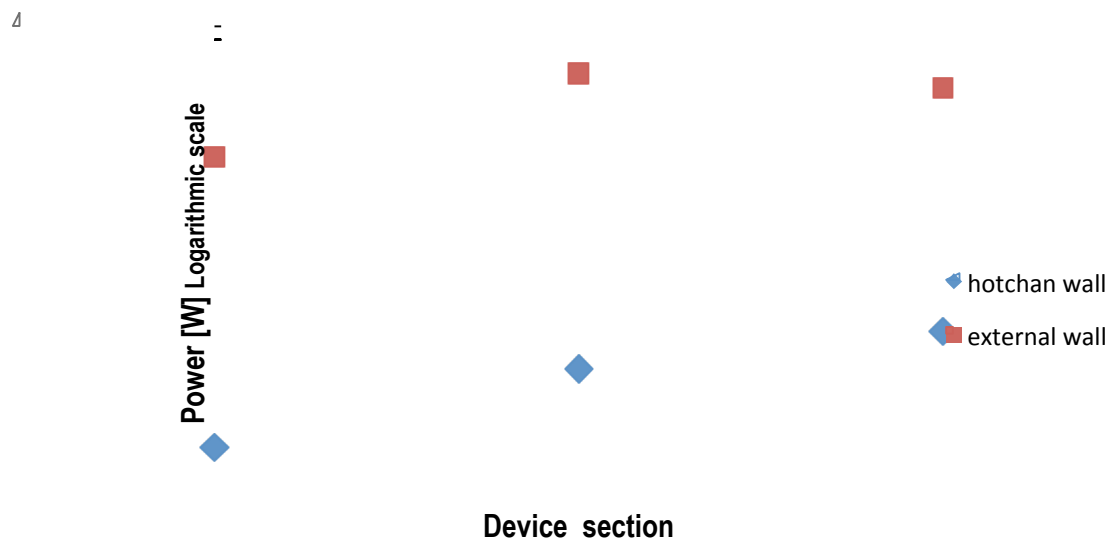
Figure 22 Power exchanged through hot and cold channel and power discharge in the surrounding, on the three sections of the device, case G5

In fig. 23 the temperature distribution of the fluid along the device for case G5 is displayed.
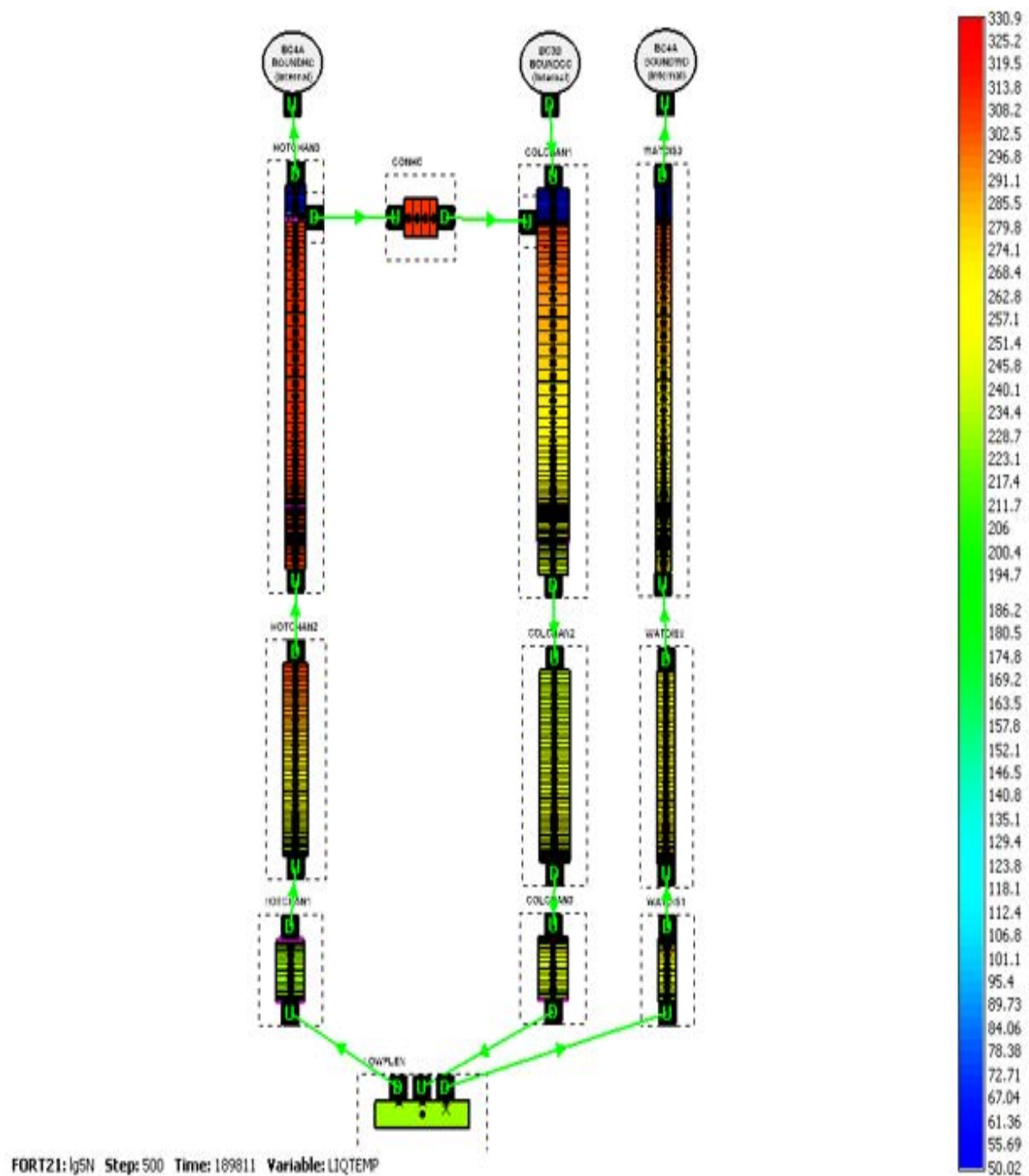
Figure 23 Temperature distribution with thermal-power on the rod and gamma-power on structures, related to the final geometry

6. APPENDIX A

In the CATHARE code a library of materials is available. In case of use of different materials the physical property must be supplied by the user in the file FWMAXX.f. In the present work the following values were used to define the physical properties, the intermediate values were calculated with a linear interpolation:

FUEL, [6]

T [°C]	Cp [J / kg K]	λ [W/ m K]	ρ[Kg/ m3]
0	240	5,96	10520,0
100	257	5,49	10500,0
200	277	5,05	10480,0
300	292	4,64	10455,0
400	302	4,27	10427,0
500	310	3,92	10398,0
600	314	3,61	10367,0
700	318	3,33	10334,0
800	320	3,08	10300,0
900	321	2,86	10264,0
1000	322	2,67	10227,0
1100	324	2,51	10188,0
1200	326	2,39	10147,0
1300	330	2,3	10105,0
1400	335	2,24	10061,0
1500	342	2,21	10016,0
1600	353	2,21	9970,0
1700	367	2,25	9922,0
1800	385	2,31	9873,0
1900	407	2,41	9822,0
2000	434	2,54	9770,0
2100	450	2,7	
2200	470	2,89	
2300	500	3,12	
2400	540	3,37	
2500	590	3,66	
2600	610	3,98	
2700	610	4,33	
2800	610	4,71	
2900	610	5,12	
3000	610	5,57	

ZIRCONIA, [7]

T [°C]	Cp [J / kg K]	λ [W/ m K]	D [m² / s]	ρ[Kg/ m3]
19,85	445	0,57	2,57E-07	4984,0
199,85	530	0,59	2,20E-07	5060,0
399,85	580	0,59	2,02E-07	5035,8
599,85	600	0,56	1,87E-07	4991,1
799,85	600	0,52	1,74E-07	4980,8
999,85	600	0,58	1,91E-07	5061,1
1199,85	610	0,79	2,57E-07	5039,2
1399,85	630	1,07	3,38E-07	5024,9
1599,85	670	1,32	3,93E-07	5013,1
1799,85	730	1,5	4,08E-07	5036,3
1999,85	820	1,85	4,50E-07	5013,6
2199,85	910	2,16	4,72E-07	5028,9
2299,85	940			
2399,85	960	2,68	5,55E-07	5030,0
2699,85	1020	3,48	6,79E-07	5024,7

POROUS ZIRCONIA, [8]

T [°C]	Cp [J / m K]	λ [W / m K]	ρ[Kg/ m3]
			480,0
93,333	543,92		
2371,1	753,12		
400		0,08	
800		0,11	
1100		0,14	
1400		0,19	
1650		0,23	

HAFNIUM, [9]

T [°C]	Cp [J / kg K]	λ [W/ m K]	ρ[Kg/ m3]
			13,31
0,05		23,3	
25,05		23	
100,05		22,4	
200,05	27,424		
400,05	29,239		
600,05	30,941		
800,05	32,552		
1000,05	34,088		
1200,05	35,564		

7. APPENDIX B

The local pressure drops was calculated by IDELCHIK HANDBOOK, [10]. The following average physical parameters in the fluid is assumed in the calculation, [11]. The pressure drop coefficients of case G5 are displayed.

P [MPa]	T [°C]	ρ [kg/m^3]	μ[Pa*s]	v [m/s]
13	330.85	638.37	$7.4196*10^{-5}$	0.1

Hot channel Inlet

  Sudden area variation.

F_0 [m^2]	F_1 [m^2]	V_0 [m/s]	Re	k	Correlation
$3,1416*10^{-4}$	$2,2902*10^{-3}$	0,054	9292	0.58796	Tab.Idelcik Pag 96
				k_{rev} 0,74447	$k=(1-F_0/F_1)^2$

Fuel inlet

  Sudden area variation.

F_0 [m^2]	F_1 [m^2]	V_0 [m/s]	Re	k	Correlation
$2,4328*10^{-4}$	$3,1416*10^{-4}$	0,069735	6300	0.25	Tab.Idelcik Pag 96
				k_{rev} 0,050904	$k=(1-F_0/F_1)^2$

End of cladding

  Sudden area variation.

F_0 [m^2]	F_1 [m^2]	V_0 [m/s]	Re	k	Correlation
$2,4328*10^{-4}$	$2,6135*10^{-4}$	0,069735	6300	0.00478	$k=(1-F_0/F_1)^2$
				k_{rev} 0,1	Tab.Idelcik Pag 96

Holes inlet

The pressure drop coefficient is calculated with two different correlation: sudden area variation and side branch in a pipe. In the code is utilized the biggest.

Sudden area variation:

Sudden area reduction

F_0 [m^2]	F_1 [m^2]	V_0 [m/s]	Re	k	Correlation
$2,0106*10^{-4}$	$2,6135*10^{-4}$	0,084378	5808	0.3	Tab.Idelcik Pag 96
				k_{rev}	$k=(1-F_0/F_1)^2$
				0,053218	

Sudden area enlargement

F_0 [m^2]	F_1 [m^2]	V_0 [m/s]	Re	k	Correlation
$2,0106*10^{-4}$	$1,6735*10^{-3}$	0,084378	5808	0.77415	$k=(1-F_0/F_1)^2$
				k_{rev}	Tab.Idelcik Pag 96
				0,75	

K_{tot}	1,0741
$K_{tot\ rev}$	0,80322

Side branch in a pipe:

F_s [m^2]	F_p [m^2]	k	Correlation
$2,0106*10^{-4}$	$2,6135*10^{-4}$	1,6646	Tab.Idelcik Pag 268
		k_{rev}	$k=(1-F_0/F_1)^2$
		0,053218	

Cold channel exit

Sudden area variation.

F_0 [m^2]	F_1 [m^2]	V_0 [m/s]	Re	k	Correlation
$1{,}0334*10^{-3}$	$2{,}29*10^{-3}$	0,016417	1966	0.30111	$k=(1-F_0/F_1)^2$
				k_{rev}	Tab.Idelcik Pag 96
				0,225	

Water discharge channel Inlet

Sudden area variation.

F_0 [m^2]	F_1 [m^2]	V_0 [m/s]	Re	k	Correlation
$7{,}068*10^{-6}$	$1{,}9761*10^{-3}$	2,4003	61955	0.49821	$k=0,5*(1-F_0/F_1)$
				k_{rev}	$k=(1-F_0/F_1)^2$
				0,99286	

8. REFERENCES

9.

[1] "Jules Horowiz Reactor, Status Report 2006-2007" – CEA

[2] "CATHARE 2 V2.5_2. – Operation Manual" CEA

[3] "CATHARE 2 V2.5_2. – Description of the Base Revision 6.1 Physical Laws Used in the 1D,0D and 3D Modules" DER/SSTH/LDAS/EM/2008-044 CEA

[4] Internal Data - CEA

[5] DRE-SRO-SIEN / Note Technique 97-143A; Annexe 1.2 - CEA

[6] Fuel Data: Phebus P.F. - Data Book FPT3-August 2007. Part 4 Material Properties - CEA

[7] Zirconia Data: Phebus P.F. - Data Book FPT3-August 2007. Part 4 Material Properties, Table at pag. 1. - CEA

[8] Porous Zirconia Data: Zircar Zirconia. Inc. It has been chosen a Zirconia Cylinder,Type : ZYC http://www.zircarzirconia.com/doc/A-G_ZYC.pdf.
NOTE: The data for Heat Capacity have been taken from Zirconia Felt,Type : ZYF http://www.zircarzirconia.com/doc/C-AB_ZYF.pdf

[9] Hafnium Data: Thermal Conductivity, Handbook of Chemistry and Physics.
Table pag E-12. CRC Press
Specific Heat Capacity, NIST website:
http://webbook.nist.gov/cgi/cbook.cgi?ID=C7440586&Units=SI&Mask=2#Thermo-Condensed
Density, http://www.periodictable.com/Elements/072/data.html

[10] "Handbook of Hydraulic Resistance"- I. E. Idelchik

[11] NIST Chemistry WebBook:
http://webbook.nist.gov/cgi/fluid.cgi?ID=C7732185&Action=Page

9. APPENDIX C

SECTION C-C
SCALE 1 : 1.2

SECTION B-B
SCALE 1 : 1.2

SECTION A-A
SCALE 1 : 1.2